sciendo

CIVIL AND ENVIRONMENTAL ENGINEERING REPORTS

E-ISSN 2450-8594

CEER 2022; 32 (2): 0023-0035
DOI: 10.2478/ceer-2022-0017
Original Research Article

RELIABILITY-BASED ASSESSMENT OF GALLOPING INSTABILITY OF THIN-WALLED STEEL BEAMS

Huu Anh Tuan NGUYEN[1]
Faculty of Civil Engineering, University of Architecture Ho Chi Minh City, Vietnam

A b s t r a c t

Galloping instability relating to cross-wind vibrations can be found in flexible and lightly damped structures. In the present paper, the reliability of a thin-walled steel beam in maintaining its galloping stability was examined using a probabilistic approach. The analysis considered random variation in the cross-sectional geometrical properties of the beam, the material elastic modulus, the structural damping and the wind speed. A large number of Monte Carlo simulations were performed with normal and Gumbel distributions applied to the random variables to determine the probability distribution function of the safety margin. The limit state is considered violated when the wind speed exceeds the onset wind velocity of galloping, resulting in the aerodynamic damping being greater than the structural damping. It was shown by a conventional codified safety factor method that the beam was robust enough for galloping stability. By contrast, the probability-based assessment revealed that the beam failed to achieve the target reliability index in case the coefficient of variation of wind speed was greater than 5%. The analysis results suggested that the code-satisfied slenderness of the beam should be reduced by a factor of 1.5-1.7 under the action of wind speed with a coefficient of variation in the range 30-40%.

Keywords: galloping instability, critical wind speed, Monte Carlo simulation, reliability index, safety factor

[1] Corresponding author: Lecturer, University of Architecture Ho Chi Minh City, 196 Pasteur Street, District 3, Ho Chi Minh City, Vietnam. E-mail: tuan.nguyenhuuanh@uah.edu.vn

1. INTRODUCTION

Galloping involves low-frequency oscillations with large amplitude in the cross-wind direction. Non circular cross sections including I, T, U and L sections are susceptible to galloping [1]. The inherent damping property of a structure often help stabilise it under wind excitation. However, if the wind speed is large enough to produce aerodynamic damping greater than the structural damping, the vibration amplitude will increase rapidly and lead to serious damage or even collapse relating to aerodynamic instability. This aerodynamic instability phenomenon can be found in slender, light-weight, lightly damped structures such as isolated structural components, iced-up cables and transmission lines, and tall buildings in case the wind speed exceeds certain critical values [2, 3]. A number of numerical and experimental studies have been carried out to investigate the effect of geometry on the transverse galloping instability. It was observed from a series of wind tunnel tests that side-surface openings could effectively enhance the galloping stability of rectangular cylinders such as box girders [4]. Testing rectangular cylinders with openings showed that the galloping onset increased with an increase in the ratio of the total opening area to the front-surface area [5]. The surface and geometric irregularities were found to have a considerable influence on the aerodynamic coefficients and hence galloping stability predictions [6]. The surface topology amplitude and wavelength could alter the galloping stability characteristics [7]. In an attempt to fill the gap in information regarding galloping instability of structures with non-rectangular cross-sections, wind tunnel testing of objects of biconvex and rhomboidal cross-section has also been performed [8]. It is necessary to adopt reasonable design solutions so that the structure does not fall into the state of galloping instability. Using tuned mass dampers was explored to increase the resistance of the structure to this type of instability [9]. Relevant literature on wind analysis of structures also includes shape optimisation of arch bridges considering statically equivalent wind load and construction stages [10].

Many construction works around the world are damaged because they have not been properly designed to resist the high wind loadings which occur in extreme events [11, 12]. Among many Asian countries heavily affected by devastating typhoons, Vietnam is one of the most social and economic vulnerable nations [13]. Vietnam is located in a region strongly affected by typhoons with many zones close to the coast experiencing high wind speeds. Due to its diverse geography, Vietnam is more vulnerable to climate change impacts including an increase in the occurrence frequency of typhoons and stormy winds. In the 2013 devastating typhoon Haiyan which struck the Philippines, Vietnam and China, the 3-s peak gust wind speed was estimated at as high as 105 m/s. The annual damage caused by wind and storms to buildings and other construction works is huge [14].

Instructions for calculating the dynamic component of wind loads are provided in the Vietnamese construction standard TCXD 229 [15]. The national technical regulation QC 02 specifies the basic wind speed according to the wind pressure zoning map and administrative zoning, serving as a basis for designing construction works subject to wind loads [16]. The conventional structural design procedure for wind actions given by several international codes including Vietnamese code is currently based on the partial safety factor approach which can be considered as a semi-probabilistic method.

This paper presents a probability-based evaluation of galloping instability of a thin-walled steel beam under wind loading. Some aspects of random variation in the material and structural properties, hence critical wind speed, as well as the applied wind speed are considered via a large number of Monte Carlo simulations in the reliability analysis. The reliability index of the beam for different levels of wind speed variation and structural slenderness are determined. A comparison with the evaluation based on the TCXD 229 safety factor is discussed. The paper also develops the required safety factor for wind speed to achieve the target reliability for different degrees of wind speed variation.

2. METHODS

2.1. Galloping instability criterion

Figure 1 shows the cross-section of a long prismatic structure under the action of a wind flow with velocity V_α at a small angle α. The structural stiffness k and damping coefficient c, in the cross-wind direction, are assumed to be constant along the length of the structure. The differential equation of cross-wind vibration is written as:

$$m\ddot{x} + c\dot{x} + kx = F_0(\alpha) \tag{2.1}$$

where m is the uniformly distributed mass of the structure and x is the cross-wind displacement of the investigated section. The aerodynamic cross-wind force per unit length $F_0(\alpha)$, in the cross-wind direction, is acquired from the lift force $F_L(\alpha)$ and drag force $F_D(\alpha)$ components [15]:

$$F_0(\alpha) = -F_D(\alpha)\sin\alpha - F_L(\alpha)\cos\alpha \tag{2.2}$$

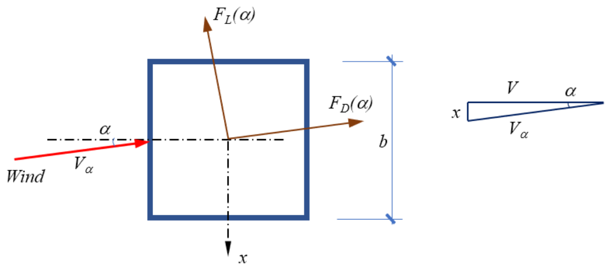

Fig. 1. Wind force acting on a body

Let ρ_a, b, $C_D(\alpha)$ and $C_L(\alpha)$ be the air density, exposure width, force coefficients in the direction of $F_D(\alpha)$ and $F_L(\alpha)$, respectively. The force $F_0(\alpha)$ can then be expressed as:

$$F_0(\alpha) = -\frac{1}{2}\rho_a V_\alpha^2 b[C_D(\alpha)\sin\alpha + C_L(\alpha)\cos\alpha] = \frac{1}{2}\rho_a V^2 b C_{DL}(\alpha) \quad (2.3)$$

in which V is the wind speed specified in the building code corresponding to the structure elevation and terrain type [16], and $C_{DL}(\alpha)$ is a combination of $C_D(\alpha)$ and $C_L(\alpha)$:

$$C_{DL}(\alpha) = -\left[C_D(\alpha)\frac{\sin\alpha}{\cos^2\alpha} + C_L(\alpha)\frac{1}{\cos\alpha}\right] \quad (2.4)$$

With α being small, $C_{DL}(\alpha)$ can be approximated by the first two terms $C_{DL}(0)$ and $C'_{DL}(0)$ of the Taylor series expansion at $\alpha = 0$ as:

$$C_{DL}(\alpha) = C_{DL}(0) + C'_{DL}(0)\frac{\dot{x}}{V} \quad (2.5)$$

The equation of motion (2.1) can subsequently be rearranged in the form:

$$\ddot{x} + 2\gamma\omega\dot{x} + \omega^2 x = \frac{1}{2m}\rho_a V^2 b C_{DL}(0) \quad (2.6)$$

where ω is the angular natural frequency with $\omega^2 = k/m$, and γ given by (2.7) can be considered as a form of damping.

$$\gamma = \frac{1}{2}\left[c - \frac{1}{2}\rho_a V^2 b C'_{DL}(0)\right] \quad (2.7)$$

A positive value of γ in (2.6) would help damp out the transverse vibration amplitude, hence preventing galloping instability. The critical wind speed in terms of galloping instability, V_{cr}, can be obtained as (2.8) by equating the damping factor γ to zero. The limit state $V = V_{cr}$ is therefore associated with a scenario when the aerodynamic damping equals the inherent structural damping, making the global damping null in the cross-wind bending mode. The empirical coefficient $C'_{DL}(0)$ in (2.8) is taken as 2.7 for a square or hollow square cross-section [15].

$$V_{cr} = \frac{2c}{\rho_a b C'_{DL}(0)} \tag{2.8}$$

2.2. Limit state function and random variables for case study beam

Figure 2 depicts the cross-section and fundamental mode shape of the case study beam which is an outdoor simply supported thin-walled steel beam. The beam has a span length of 10 m. The hollow square cross-section has a nominal width of b = 220 mm and thickness of t = 2.5 mm. The beam is subjected to a wind flow with the codified characteristic (basic) wind speed at the structure elevation for a 50-year reference period of V_k = 34.59 m/s. The steel material has a mass density of ρ_s = 7850 kg/m^3 and modulus of elasticity of E = 2×10^5 MPa. The structural damping ratio ζ has a nominal value of 1%.

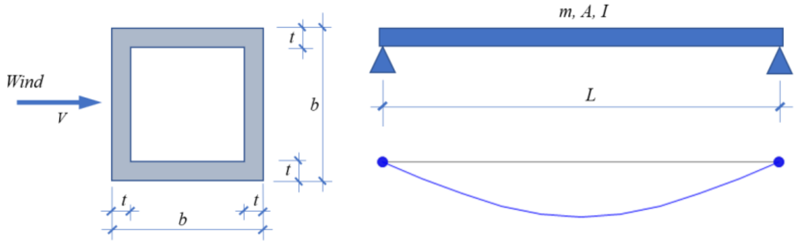

Fig. 2. Cross-section and mode shape of case study beam

For a probabilistic evaluation of galloping instability of the beam, the limit state function is introduced as:

$$g(X) = V_{cr} - V \tag{2.9}$$

where the vector of basic random variables X includes the area A and moment of inertia I of the cross-section, material modulus of elasticity E, structural damping ratio ζ, and the wind speed V for a design working life of 50 years. Table 1 presents the statistical properties of the random variables, which are essentially based on European guidelines on structural reliability [17, 18].

The normal distribution can be used for geometry steel sections and material properties with low variation [18]. On the other hand, the Gumbel distribution, which is one of the most commonly used models of wind speed variation, uses an exponential shape to describe the distribution of extreme values of the wind speed [19]. The probability density function of wind speed was expressed in the form:

$$\varphi(V) = s\exp\{-s(V - V_{mod}) - \exp[-s(V - V_{mod})]\} \qquad (2.10)$$

where both the parameters V_{mod} and s of the Gumbel distribution can be determined from the mean μ_V and standard deviation σ_V [17]:

$$V_{mod} = \mu_V - 0.577\frac{\sqrt{6}\,\sigma_V}{\pi} \qquad (2.11)$$

$$s = \frac{\pi}{\sqrt{6}\,\sigma_V} \qquad (2.12)$$

Table 1. Statistical properties of random variables

Variable, X	Dimension	Mean, μ_X	Standard deviation, σ_X	Distribution
A	m^2	$b^2 - (b - 2t)^2$	$0.02\mu_X$	Normal [18]
I	m^4	$(b^4 - (b - 2t)^4)/12$	$0.02\mu_X$	Normal [18]
E	N/m^2	2×10^{11}	$0.04\mu_X$	Normal [18]
ζ		0.01	$0.1\mu_X$	Normal [15]
V (50 years)	m/s	$0.7V_k$	$0.35\mu_X$	Gumbel [17]

2.3. Monte Carlo simulation and reliability evaluation

Despite requiring high computational effort, Monte Carlo simulation is an efficient method for reliability evaluation of complex engineering structures [20-24]. In this paper, the reliability analysis of galloping stability of the beam was performed using a large number of Monte Carlo simulations. Firstly, independent random values of the variables A, I, E, ζ and V with statistical properties acquired from Table 1 were generated by a MATLAB code. The mass per unit length of the beam was computed as $m = A\rho_s$. The natural frequency f and structural damping coefficient c associated with the fundamental vibration mode were obtained using formulae (2.13) and (2.14) respectively [1]. The critical wind speed V_{cr} as per (2.8) can then be determined. Subsequently, the limit state function $g(X)$, or safety margin $M = V_{cr} - V$, was evaluated.

$$f = \frac{\pi}{2}\sqrt{\frac{EI}{mL^4}} \qquad (2.13)$$

$$c = 2m\omega\zeta = 4\pi mf\zeta \qquad (2.14)$$

This random simulation process was repeated for 5 million times, allowing determination of statistical properties of the safety margin. The measure of reliability can be identified with the reliability index β which is the ratio of the mean to the standard deviation of the safety margin [25].

The safety of a structure is considered satisfactory when the reliability index of the structure is not less than the target reliability index. Recommended minimum values for reliability index are given in building codes and standards [25, 26] which consider different levels (high, medium, low) of the consequences of structural failure or malfunction. The target reliability index for a 50-year reference period of the studied beam can be taken as 3.80, which corresponds to medium consequence for loss of human life, considerable economic, social or environmental consequences [25].

3. RESULTS AND DISCUSSION

3.1. Evaluation using codified safety factor design approach

It would be useful to first present the results of the galloping instability evaluation of the beam based on the codified safety factor design method which is familiar to the practicing engineers. For a design working life of 50 years, a safety factor of 1.2 according to TCXD 229 [15] was applied to the basic wind speed to obtain the design wind speed:

$$V = 1.2V_k = 41.51 \text{ m/s} \tag{3.1}$$

The cross-sectional area and moment of inertia computed from the nominal width and thickness of the beam section were A = 2.175×10^{-3} m^2 and I = 1.715×10^{-5} m^4. The mass per unit length, fundamental frequency and structural damping coefficient were found to be m = 17.074 kg/m, f = 7.041 Hz and c = 15.106 Ns/m^2 respectively. Putting ρ_a = 1.225 kg/m^3, $C'_{DL}(0)$ = 2.7, b = 0.22 m into equation (2.8) yielded the critical wind speed of V_{cr} = 41.52 m/s. Since $V < V_{cr}$ the safety factor approach confirmed the beam adequacy for galloping stability.

3.2. Evaluation using probabilistic approach

Figure 3 illustrates the probability density functions (PDFs) of the cross-sectional area A, moment of inertia I, material modulus of elasticity E and structural damping ratio ζ randomly generated in 5 million simulations. Figure 4 depicts the PDFs of the resultant critical wind speed V_{cr} and the Gumbel-distributed wind speed V when the coefficient of variation ν of the wind speed was taken as 0.35 and the mean wind speed was $0.7V_k$ = 24.21 m/s (Table 1). The two PDF plots of V_{cr} and V are clearly seen to partly overlap and the PDF plot of the safety margin contains a considerable area of negative values (Fig. 4). Indeed, the probability of failure was found to be 0.0489. The mean and standard deviation of the limit state function were predicted to be 17.288 and 9.500 m/s respectively, resulting a reliability index β of 1.820 which is less than the recommended target value of 3.80. Therefore, the beam would be deemed unsatisfactory when galloping instability is of concern.

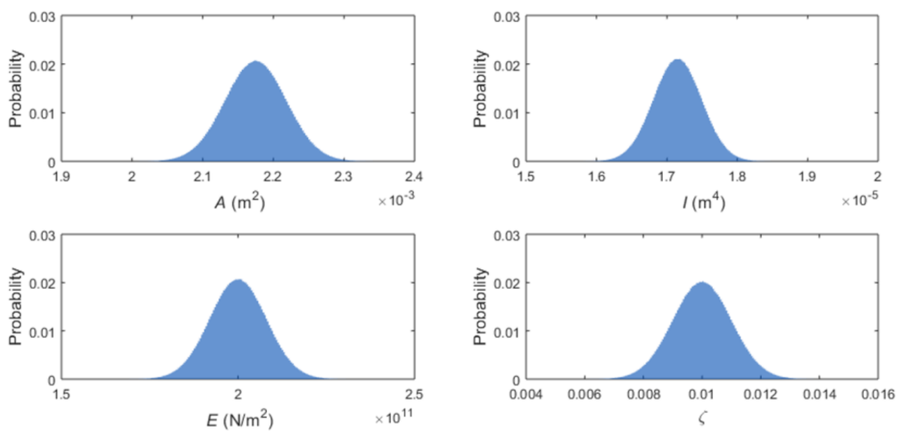

Fig. 3. PDFs of A, I, E and ζ for beam with b = 220 mm

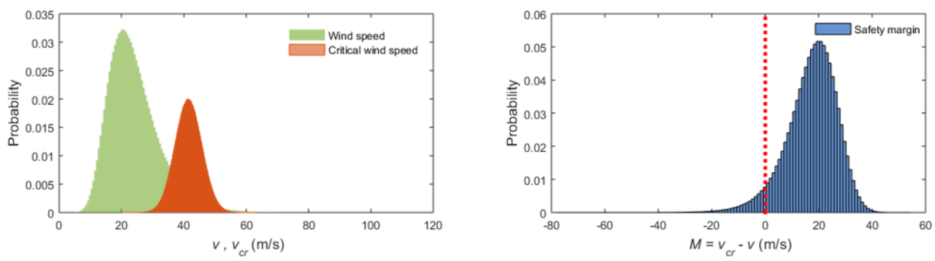

Fig. 4. PDFs of wind speed and safety margin for b = 220 mm, ν = 0.35

3.3. Effect of beam slenderness and wind speed variation on reliability

Further investigations were performed for beam width b of 220, 235, 250, 275, 300, 325, 350 and 375 mm and coefficient of variation of wind speed ν of 0.05, 0.10, 0.15, 0.20, 0.25, 0.30, 0.35 and 0.40. The analysis for each combination of b and ν involved 5 million Monte Carlo simulations similar to those discussed previously. Figure 5 shows the PDFs of V_{cr}, V and safety margin for ν = 0.35 when b was increased to 350 mm. The corresponding reliability index was found to be 3.885 which guaranteed the target reliability and was 2.1 times greater than that obtained from b = 220 mm. The curves plotted in Fig. 6 allow determination of the reliability index β for various combinations of b and ν. It can be seen that the original beam with b = 220 mm would achieve the target reliability when ν was equal to just 0.05 rather than 0.35. An increase in the original beam width by a factor of 1.5-1.7 was needed to avoid galloping instability relating to coefficient of variation of wind speed in the range 30-40%.

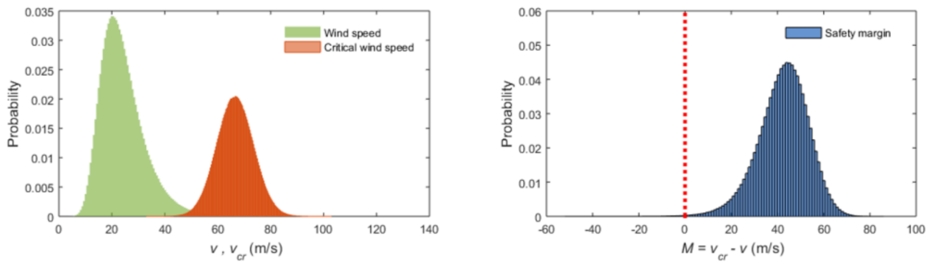

Fig. 5. PDFs of wind speed and safety margin for b = 350 mm, ν = 0.35

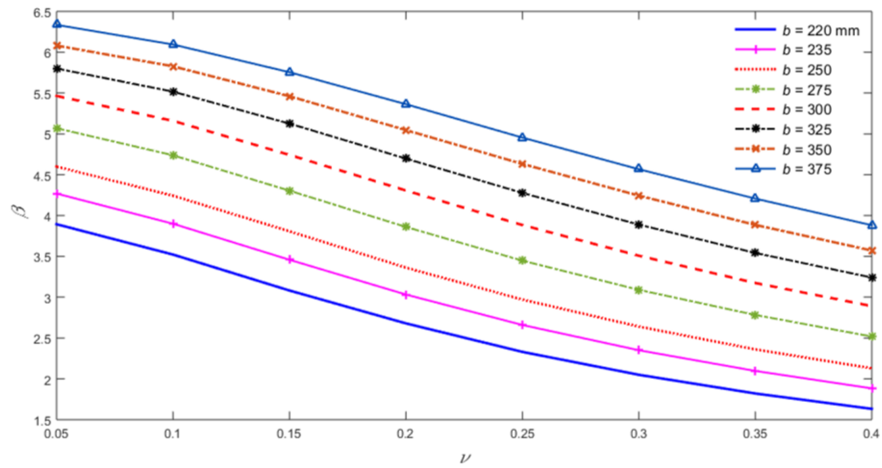

Fig. 6. Reliability index versus coefficient of variance of wind speed for different beam sizes

The slenderness ratio of the beam is now defined as $\lambda = L/b$. Table 2 presents the combinations λ and ν that would result in a reliability index greater than the recommended target value of 3.80 and hence a satisfactory beam. For instance, if the wind speed has ν = 0.2 then a reliability index of 3.86 can be acquired for the beam with $\lambda = 36.4$ (L = 10 m, b = 275 mm). The greater the wind speed variation, the lower the required slenderness of the beam.

Table 2. Beam slenderness and wind speed coefficient of variation for galloping stability

λ	45.5	42.6	40.0	36.4	33.3	30.8	28.6	26.7
ν	0.05	0.10	0.15	0.20	0.25	0.30	0.35	0.40
β	3.894	3.899	3.807	3.860	3.883	3.889	3.885	3.881

3.4. Back analysis for determination of required safety factor

This section suggests the required safety factor for wind speed to apply to the basic wind speed V_k in the conventional safety factor method, corresponding to different degrees of wind speed variation.

As found previously, when the beam width b was increased from 220 to 375 mm in response to ν increasing from 0.05 to 0.40, the target reliability index of 3.80 was achieved. Table 3 presents the critical wind speed V_{cr} calculated using equation (2.8) with b = 220-375 mm, t = 2.5 mm, L = 10 m, $E = 2\times10^5$ MPa, ζ= 0.01, ρ_s = 7850 kg/m^3, ρ_a = 1.225 kg/m^3 and $C'_{DL}(0)$ = 2.7. Letting the design wind speed V be equal to V_{cr}, the safety factor for wind speed, which is defined as V/V_k, can be computed as $n = V_{cr}/V_k$. As can be seen from Table 3, for $\nu = 0.35$ the beam should be designed with a safety factor being 1.6 times greater than the code-specified value of 1.2.

Table 3. Back calculation of safety factor for wind speed

ν	0.05	0.10	0.15	0.20	0.25	0.30	0.35	0.40
b (mm)	220	235	250	275	300	325	350	375
V_{cr} (m/s)	41.52	44.42	47.31	52.14	56.96	61.79	66.62	71.44
n	1.20	1.28	1.37	1.51	1.65	1.79	1.93	2.07

A plot of the required safety factor n versus coefficient of variation of wind speed ν is shown in Fig. 7. A simple linear regression trendline with the coefficient of determination R^2 of as high as 0.9921 can be found as:

$$n = 2.5382\nu + 1.0269 \tag{3.2}$$

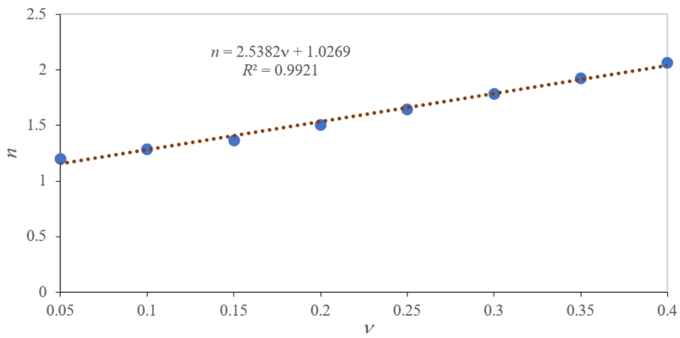

Fig. 7. Safety factor versus coefficient of variation of wind speed

4. CONCLUSION

Long thin-walled steel beams which possess high flexibility and low damping could be prone to galloping instability relating to the large amplitude, low frequency oscillation of the structures in the direction transverse to the mean wind direction. Using a probabilistic approach, the paper discussed some findings on the dependence of the aerodynamic stability reliability on the beam size and wind load variation.

The case study beam with a width of 220 mm and slenderness ratio of 45.5 was found to satisfy the criterion of galloping stability when evaluated according to the conventional codified safety factor method. However, the full probabilistic analysis showed that these size and slenderness could guarantee the recommended reliability level only when the coefficient of variation of wind speed was 0.05. In case the coefficient of variation of wind speed is as high as 0.35 as suggested in the relevant literature, an increase in the width or a decrease in the slenderness by a factor of 1.59 would be essential in order for the beam to achieve a reliability index of 3.80 for a 50-year reference period.

Structural engineers may be familiar with the safety factor method rather than the full probabilistic analysis. However, a design of the case study beam based on the traditional safety factor method should take the safety factor for wind speed in the range 1.20 to 2.07 corresponding to the coefficient of variation of wind speed from 0.05 to 0.40, instead of using a single safety factor of 1.2.

REFERENCES

1. EN 1991-1-4:2005 2010. *Eurocode 1: Actions on structures - Part 1-4: General actions - Wind actions*. Brussels: European Committee for Standardization.

2. Piccardo, G, Pagnini, LC and Tubino, F 2015. Some research perspectives in galloping phenomena: critical conditions and post-critical behavior. *Continuum Mechanics and Thermodynamics* **27**, 261-285.
3. Alonso, G, Meseguer, J, Sanz-Andrés, A and Valero, E 2010. On the galloping instability of two-dimensional bodies having elliptical cross-sections. *Journal of Wind Engineering and Industrial Aerodynamics* **98**, 438-448.
4. Wang, J, Hu, J and Ma, K 2016. Wind speed probability distribution estimation and wind energy assessment. *Renewable and Sustainable Energy Reviews* **60**, 881-899.
5. Wang, J, Yagi, T, Ushioda, J, Ichikawa, H, Yamamoto, S and Noguchi, K 2020. Side-surface openings effects on galloping instability for a rectangular cylinder. *Journal of Wind Engineering and Industrial Aerodynamics* **206**, 104303.
6. Demartino, C and Ricciardelli, F 2018. Assessment of the structural damping required to prevent galloping of dry HDPE stay cables using the quasi-steady approach. *Journal of Bridge Engineering* **23 (4)**, 04018004.
7. Feero, MA, Naguib, AM and Koochesfahani, M 2020. Effect of surface topology on the galloping instability of rectangular cylinders. *International Journal of Heat and Fluid Flow* **86**, 108721.
8. Alonso, G, Valero, E and Meseguer, J 2009. An analysis on the dependence on cross section geometry of galloping stability of two-dimensional bodies having either biconvex or rhomboidal cross sections. *European Journal of Mechanics-B/Fluids* **28 (2)**, 328-334.
9. Mannini, C et al. 2016. Aeroelastic stability of two long-span arch structures: A collaborative experience in two wind tunnel facilities. *Engineering Structures* **119**, 252-263.
10. Pouraminian, M and Ghaemian, M 2015. Shape optimisation of concrete open spandrel arch bridges. *Građevinar* **67**, 1177-1185.
11. Chmielewski, T, Szer, J and Bobra, P 2020. Derecho wind storm in Poland on 11–12 August 2017: results of the post-disaster investigation. *Environmental Hazards* **19 (5)**, 508-528.
12. Masoomi, H, Ameri, MR and van de Lindt, JW 2018. Wind performance enhancement strategies for residential wood-frame buildings. *Journal of Performance of Constructed Facilities* **32 (3)**, 04018024.
13. Nguyen, KA, Liou, YA and Terry, JP 2019. Vulnerability of Vietnam to typhoons: A spatial assessment based on hazards, exposure and adaptive capacity. *Science of the Total Environment* **682**, 31-46.
14. Yang, Q, Gao, R, Bai, F, Li, T and Tamura, Y 2018. Damage to buildings and structures due to recent devastating wind hazards in East Asia. *Natural Hazards* **92**, 1321–1353.

15. TCXD 229:1999. *Guidance for determination of dynamic component of the wind loads under TCVN 2737:1995* (*in Vietnamese*). Hanoi: Vietnamese Construction Standard.
16. QCVN 02:2009/BXD. *National Technical Regulation on Natural Physical and Climatic Data for Construction* (*in Vietnamese*). Hanoi: Vietnamese Construction Regulation.
17. Leonardo Da Vinci Pilot Project CZ/02/B/F/PP-134007 2005. *Implementation of Eurocodes handbook 2: reliability backgrounds*. Prague.
18. Markova, J, Sousa, M, Dimova, S, Athanasopoulou, A, Iannaccone, S and Pinto, A 2018. *Reliability of structural members designed with the Eurocodes NDPs selected by EU and EFTA member states*. EUR 29410 EN Publication by European commission and joint research center.
19. Wang, J, Hu, J and Ma, K 2016. Wind speed probability distribution estimation and wind energy assessment. *Renewable and Sustainable Energy Reviews* **60**, 881-899.
20. Thomopoulos, NT 2013. *Essentials of Monte Carlo simulation: Statistical methods for building simulation models*. New York: Springer Science and Business Media.
21. Pouraminian, M et al. 2020. Reliability-based safety evaluation of the BISTOON historic masonry arch bridge. *Civil and Environmental Engineering Reports* **30 (1)**, 87-110.
22. Pouraminian, M, Pourbakhshian, S and Noroozinejad Farsangi, E 2020. Reliability assessment and sensitivity analysis of concrete gravity dams by considering uncertainty in reservoir water levels and dam body materials. *Civil and Environmental Engineering Reports* **30 (1)**, 1-17.
23. Rahgozar, N, Pouraminian, M and Rahgozar, N 2021. Reliability-based seismic assessment of controlled rocking steel cores. *Journal of Building Engineering* **44**, 102623.
24. Pouraminian, M 2022. Multi-hazard reliability assessment of historical brick minarets. *Journal of Building Pathology and Rehabilitation* **7 (1)**, 1-12.
25. EN 1990:2002 2005. *Eurocode - Basis of Structural Design*. Brussels: European Committee for Standardization.
26. ISO 2394:2015 2015. *General Principles on Reliability for Structures*. Geneva: International Standards Organization.

Editor received the manuscript: 25.01.2022